

Measuring the Refractive Index of Infrared Materials by Dual-Wavelength Fabry-Perot Interferometry

A Senior Project

presented to

the Faculty of the Physics Department

California Polytechnic State University, San Luis Obispo

In Partial Fulfillment

of the Requirements for the Degree

Bachelor of Science

by

Griffin Taylor

June, 2013

Advisor, Dr. Glen D. Gillen

Introduction:

The index of refraction of a material is what governs how light passes through that material. We notice the index of refraction at work when we look through a glass of water, at a rainbow, or at the dispersion of light through a prism. The refractive index tells us the focusing power of a lens, how a prism will disperse light, and we use it to differentiate between materials. In semiconductor crystals, a precise measurement of the linear index of refraction is required to predict nonlinear properties of the crystal [1].

The definition of the index of refraction is that it is the ratio of speed of light in a vacuum over the speed of light in the medium. Light changes speed when it passes between different media; this is why light bends when it moves from one medium to another at an angle other than the normal [2]. The index of refraction depends on the wavelength of the light; this is illustrated by Fig. 1 as white light passes through a prism. Dispersion is demonstrated as light with shorter wavelength deviates farther from the original path than light with a longer wavelength.

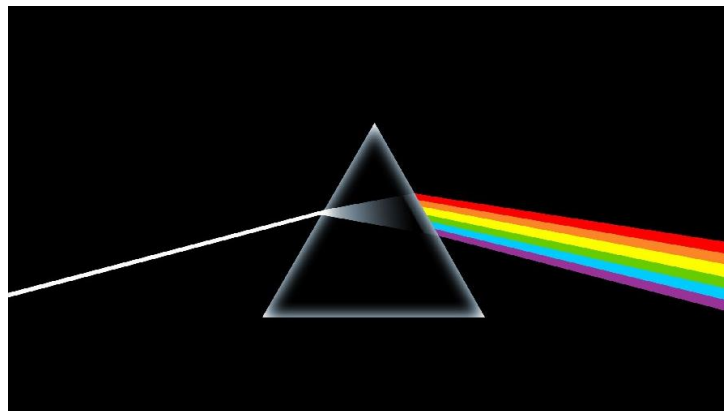


Figure 1 – Collimated white light through a prism.¹

¹ http://upload.wikimedia.org/wikipedia/en/thumb/3/3b/Dark_Side_of_the_Moon.png/220px-Dark_Side_of_the_Moon.png

An historical way to measure the refractive index of a material is called the minimum deviation method. It involves carving out a prism of the material and measuring how much the light bends from its original path when it passes through that prism. This method is exceptionally accurate and is ideal for measuring the index of refraction of materials. However, it requires there to be enough of the material to shape into a prism, so it is unfeasible for some infrared materials [3]. For instance, when the sample is a thin wafer measuring only a few millimeters in thickness, which is common for infrared semiconductor materials, a different method is needed.

Semiconductors are grown in cylindrical boules, and then cut into thin wafers. They are often formed with a concentration of elements that varies as a function of position within the boule, thus they are not uniform throughout. The index of refraction varies when the concentration of the different elements varies [3]. So, a boule which is not uniform makes measuring the index of refraction of each of the wafers necessary. There are several methods that have been developed to measure the index of refraction of such wafers, and by necessity they are non-destructive. Each method uses interferometry as the means for their measurement of the refractive index.

The first of these nondestructive methods uses a Michelson interferometer to measure the index of refraction of a thin wafer. The Michelson is especially good at measuring a slight difference in phase of electromagnetic waves, but it is used here to measure the index of refraction of a sample with parallel sides [3]. The advantages of this method are that it is nondestructive and yields a measurement for the index of refraction with an accuracy of 10^{-3} [3]. The precision of this measurement is limited by the precision of the measurement of the thickness of the material. With a wafer that is a few millimeters thick, it is difficult to measure

the thickness beyond the micron level [3]. Another factor that boosts uncertainty for the Michelson interferometer is its sensitivity to vibrations and air currents [4].

A recently developed method which allows for the measurement of the index of refraction of semiconductor wafers is an adaptation to the Michelson interferometer that combines both Michelson and Fabry-Perot interferometry [4]. The thickness of the wafer and the index of refraction can be decoupled by using information from Michelson interference and Fabry-Perot interference which are joined together in one experimental setup. The index of refraction was reliably calculated with an accuracy of 10^{-3} or better [4]. This is a remarkable example of where theory and experimental innovation meet to solve an open challenge – in this case measuring the refractive index of semiconductor wafers.

The most recent technique uses Fabry-Perot interferometry exclusively, and it employs two lasers of different wavelength to decouple the refractive index and the thickness of the wafer [1]. An advantage of using Fabry-Perot interferometry exclusively is that it is not as affected by vibrations and air currents as the Michelson interferometer. This approach also reduces the time of the experiment, as only one scan is needed to collect the data required to decouple the index of refraction and the thickness of the wafer. Furthermore, each scan yields two values for the index of refraction: one for each wavelength of light. This increases the speed at which a dispersion curve can be crafted. The dispersion curve gives the relationship between a material's index of refraction and different wavelengths of light. Finally, the dual-wavelength Fabry-Perot experiment yields an accuracy of 10^{-5} [1]. This level of precision aides in the theoretical predication of the semiconductor's nonlinear optical behavior [3].

This project serves as a proof of theory for the dual-wavelength Fabry-Perot interferometric method that Choi, *et al.* [1] employed to measure the index of refraction of thin

wafers. It builds on a project started by Czapla [5] and reports on the results that we observed which were consistent with what is expected from Fabry-Perot interference. Namely, the light of our lasers formed an interference pattern which we observed. We measured the intensity of a segment of the pattern which oscillated as a function of the incident angle of the light. Furthermore, the lasers of different wavelength oscillated at different frequencies, which is consistent with the theory of Fabry-Perot interference.

Theory:

The speed that light travels in an isotropic material is derived from Maxwell's equations in a medium [6]. We define the index of refraction, n , to be

$$n = \sqrt{\frac{\mu\epsilon}{\mu_0\epsilon_0}} \quad (1)$$

where μ_0 is the permeability of free space, ϵ_0 is the permittivity of free space, μ is the permeability of the material, and ϵ is the permittivity of the material. With this definition, we find that the index of refraction can be written in terms of the speed of light in a vacuum, c , and the speed of light in the material, v , as

$$n = \frac{c}{v} . \quad (2)$$

In this experiment, we treat light as a monochromatic plane wave with an electric field that oscillates perpendicular to the direction of travel. The electric field of this plane wave is of the form

$$\vec{E} = E_0 e^{i(kz - \omega t + \varphi)} \hat{x} \quad (3)$$

where E_0 is the initial amplitude of the electric field, k is the wave number, z is the position on the optical path, ω is the angular frequency, t is the time, φ is the phase constant, and \hat{x} is the polarization dimension [2]. The terms inside the parentheses in Eq. (3) are referred to as the phase. Because the lasers we used have a very narrow bandwidth, we can approximate their light as monochromatic. Furthermore, the laser output was well-collimated, so our approximation of it as a plane wave is valid.

Fabry-Perot interference occurs when a plane wave passes through a material with parallel sides at an angle other than the normal [2]. This is also known as thin-film interference, which is shown in Fig. 2. The interference occurs when the transmitted light waves, which have different phases, recombine. Figure 2 illustrates how the light travels through a thin film of refractive index, n . As observed in Fig. 2, there are multiple internal reflections in the film, which lead to many reflected and transmitted waves. The reflected waves are $R_0, R_1, R_2, \dots, R_n$, and the transmitted waves are T_1, T_2, \dots, T_n . The angle of refraction is θ_t , and the thickness is d .

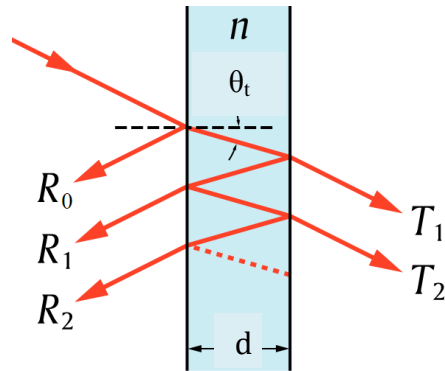


Figure 2 – Reflected and transmitted paths for light incident upon a thin film.²

² <http://upload.wikimedia.org/wikipedia/en/3/39/Etalon-2.svg>

We measured the intensity of the light, which is proportional to the magnitude of the electric field squared [2]. The intensity of the light transmitted through an etalon can be found to be

$$I_T = \left[\frac{(1 - r^2)^2}{1 + r^4 - 2r^2 \cos \delta} \right] I_i \quad (4)$$

where I_T is the intensity of the transmitted light, r is the reflection coefficient, δ is the phase difference, and I_i is the intensity of the incident light [2]. The intensity of the transmitted light is dependent on the phase difference, δ , between successive transmitted beams and is given by

$$\delta = k\Delta. \quad (5)$$

The optical path length difference, Δ , is given by

$$\Delta = 2nd \cos \theta_t \quad (6)$$

where n is the index of refraction of the etalon (or plate), d is the thickness of the plate, and θ_t is the angle of refraction. The phase difference, δ , is dependent on the index of refraction, n , which is contained in the optical path difference. The wavenumber, k , is the that of light in vacuum, or

$$k = \frac{2\pi}{\lambda}. \quad (7)$$

Therefore, we express the phase difference as

$$\delta = \frac{4\pi d}{\lambda} n \cos \theta_t, \quad (8)$$

which can be rewritten using the trigonometric identity for any angle, φ ,

$$\cos(\varphi) = \sqrt{1 - \sin^2(\varphi)}, \quad (9)$$

to be

$$\delta = \frac{4\pi d}{\lambda} \sqrt{n^2 - n^2 \sin^2 \theta_t}. \quad (10)$$

By applying Snell's Law,

$$n \sin(\theta_t) = n_i \sin(\theta_i), \quad (11)$$

where n_i is the index of refraction of the incident medium and θ_i is the incident angle, Eq. (10) can be rewritten in terms of the incident angle. We take n_i to be equal to 1, as it is the index of refraction of air in this case, which results in

$$\delta = \frac{4\pi d}{\lambda} \sqrt{n^2 - \sin^2 \theta_i}, \quad (11)$$

which gives the phase difference in terms of the thickness of the plate, d , the wavelength of the light passing through the plate, λ , the index of refraction of the plate, n , and the angle from the normal of the incident light, θ_i [2].

According to Eq. (11) the phase difference will have maxima, minima, and everything in between when the angle of incident light is rotated. Notice from Eq. (4) that the cosine of the phase difference oscillates between -1 and 1 when the phase difference itself changes. This in turn results in the oscillation of the transmitted intensity. Furthermore, we expect from Eq. (11) that the transmitted intensity of light with a particular wavelength oscillates at a different frequency than that of light of a different wavelength because the phase difference is dependent on the wavelength.

Experimental Design:

This project continues an ongoing experiment which serves as a proof of theory for the dual-wavelength Fabry-Perot interferometric method which measures the refractive index and thickness of thin wafers with parallel sides. This technique uses two lasers of different

wavelength which travel collinearly through the same etalon. Figure 3 shows the experimental setup of Choi, *et al.*, who first published their work on this experiment in 2010 [1].

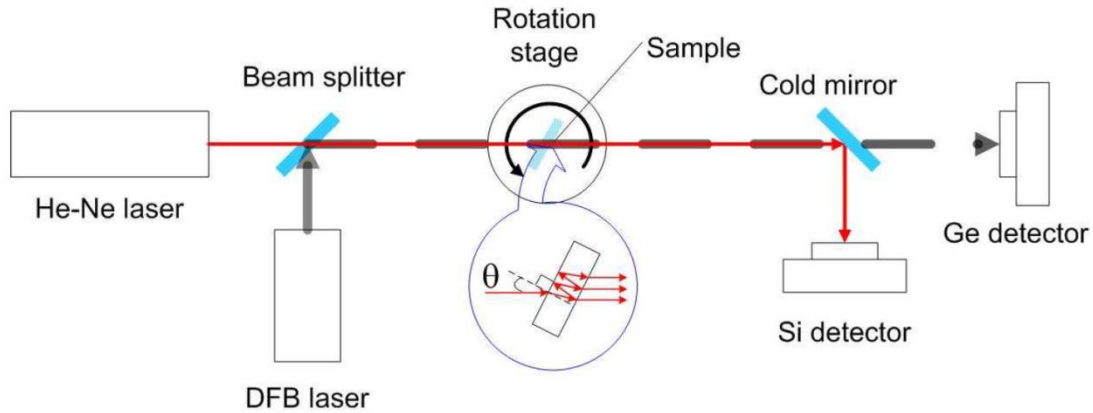


Figure 3 – Experimental setup of the dual-wavelength Fabry-Perot interferometer [1].

Our experimental setup, which was previously developed by Czapla [5], is shown in Fig. 4 and Fig. 5. Silvered mirrors guide the two lasers, a 780-nm laser (shown in blue) and a 1310-nm diode laser (shown in red), to converge as they pass through a sample of infrared material, which is mounted on the rotation stage. After they pass through the sample, each laser is guided through a 100 μ m pinhole into a detector which measures the intensity of the light.

Each detector is wired into an analog-to-digital converter, DAQ, which is a useful addition to this experiment. It allows for a faster acquisition of data as compared to the lock-in amplifier. The DAQ takes the analog signal of the detector and converts it to a digital signal which LabVIEW reads, records, and analyzes. The lasers are aligned to be approximately collinear inside the sample. The reason that the lasers are offset slightly is because it allows their outputs to reach separate detectors and to bypass the requirement of having a specialized mirror which transmits one laser and reflects the other. The advantage to this setup is that the lasers can be changed out without needing a specialized mirror for each combination.

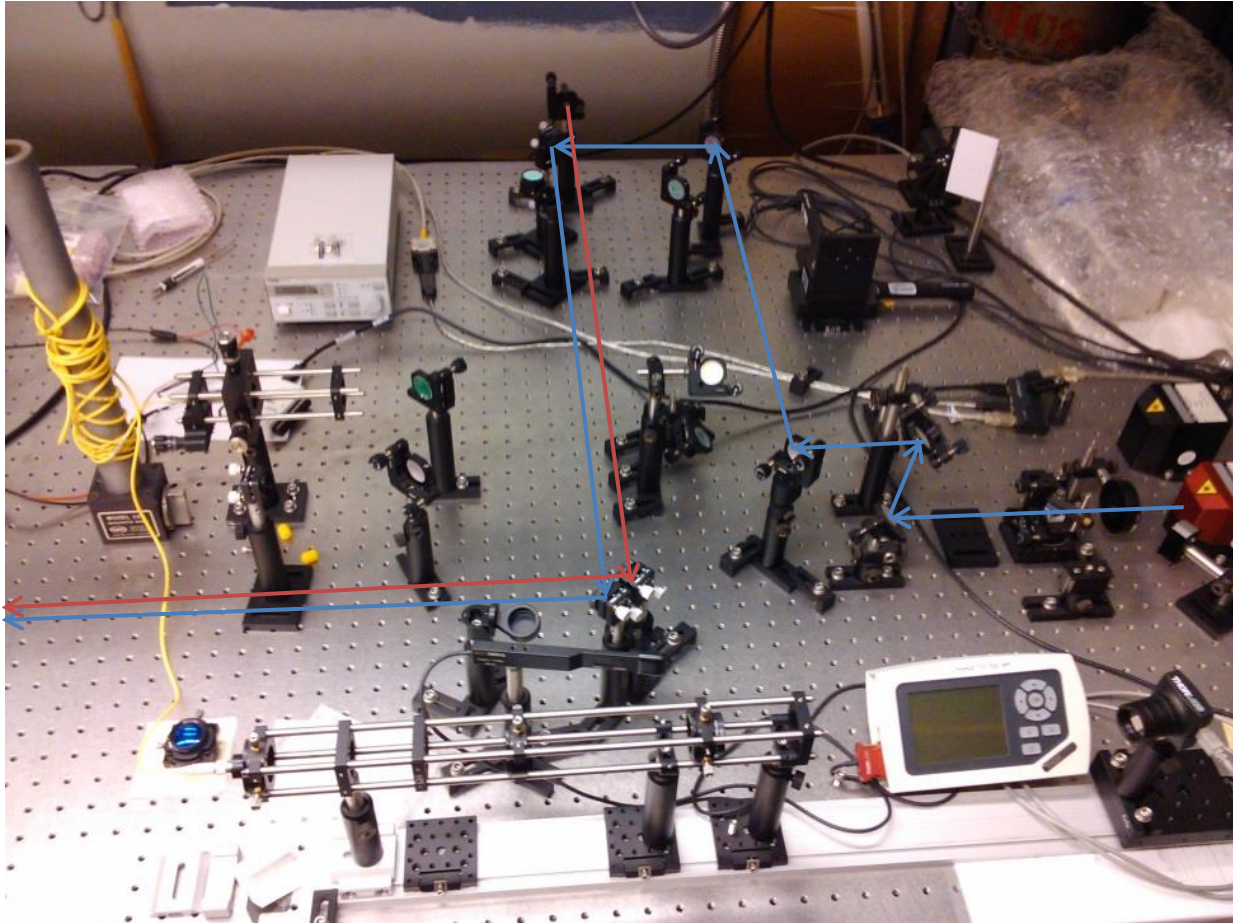


Figure 4 – The laser paths of the 780-nm laser (blue) and the 1310-nm diode laser (red).

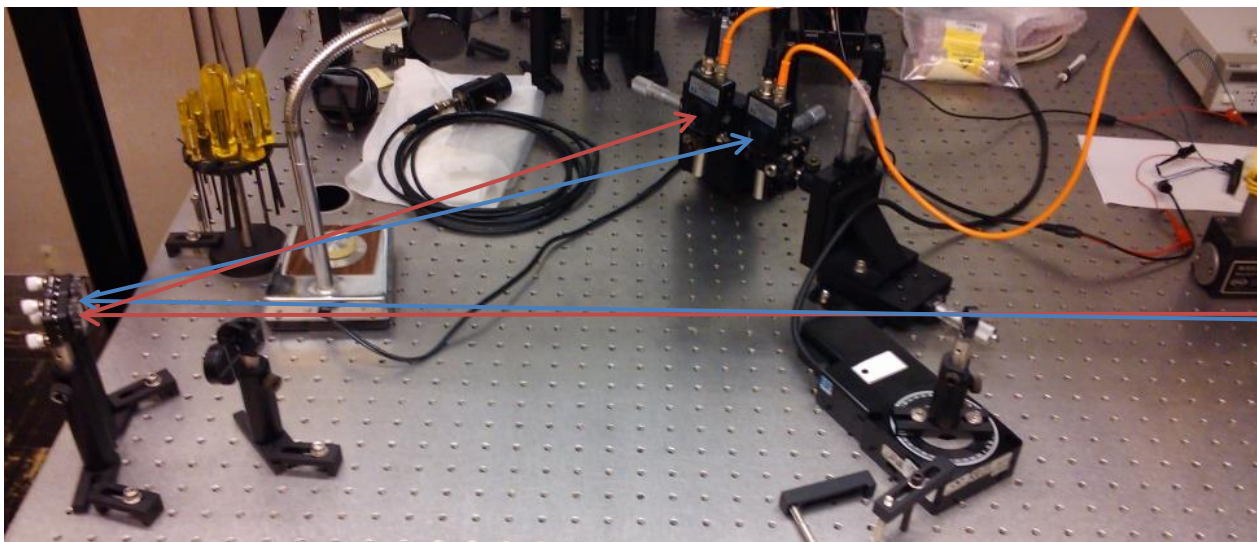


Figure 5 – The laser paths of the 780-nm laser (blue) and the 1310-nm diode laser (red).

Part of the process of this project was gaining familiarity with LabVIEW. LabVIEW has an excellent tutorial for getting started in the LabVIEW help files. Furthermore, there is a useful tutorial on the DAQ assistant, which helped me construct a virtual instrument, VI, for the DAQ. I built the block diagram seen in Fig. 6 with the tools and guidance found in the help files. This block diagram governs the VI which reads the signals from the DAQ and writes them to an excel file. It also graphs the signals for a helpful visual seen in Fig. 7. The VI also controls whether LabVIEW takes a single set of data or runs continuously.

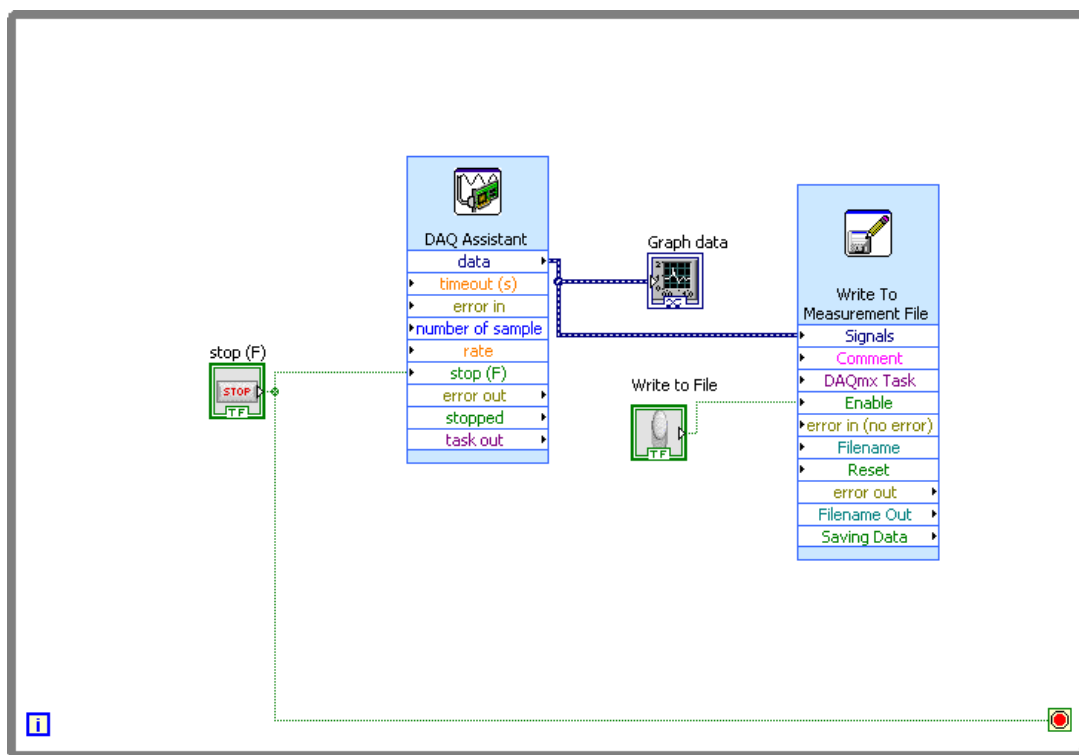


Figure 6 – LabVIEW block diagram for the DAQ.

Figure 7 shows the VI after I took a full set of data. The 1310-nm diode laser is represented in red, and the 780-nm laser is represented in green. Both lasers are plotted on the graph of the intensity versus the data point. The DAQ assistant controls the number of points to acquire, the data acquisition rate, the range of the input signal, and other properties. This particular plot in Fig. 7 took 25,000 samples at 1000 samples per second, and the rotation speed of the motion controller was 2 degrees per second. The DAQ assistant's properties page which allows me to change these settings is shown in Fig. 8.

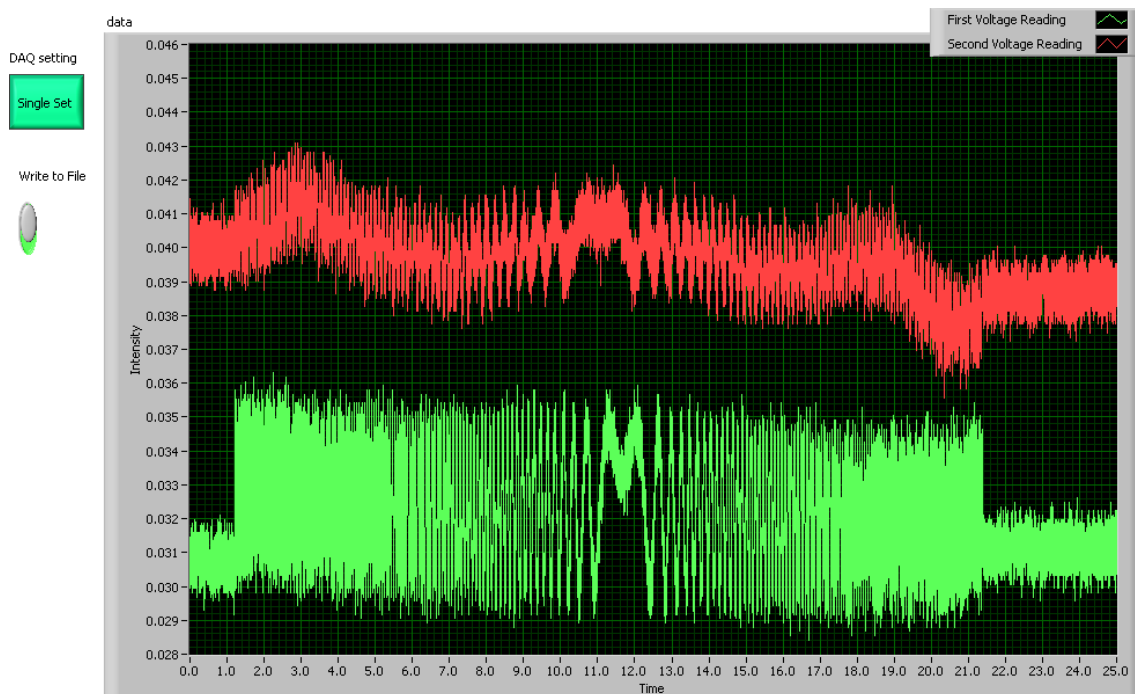


Figure 7 – LabVIEW VI illustrating the signal output of the detectors for the 780-nm laser (green) and the 1310-nm diode laser (red).

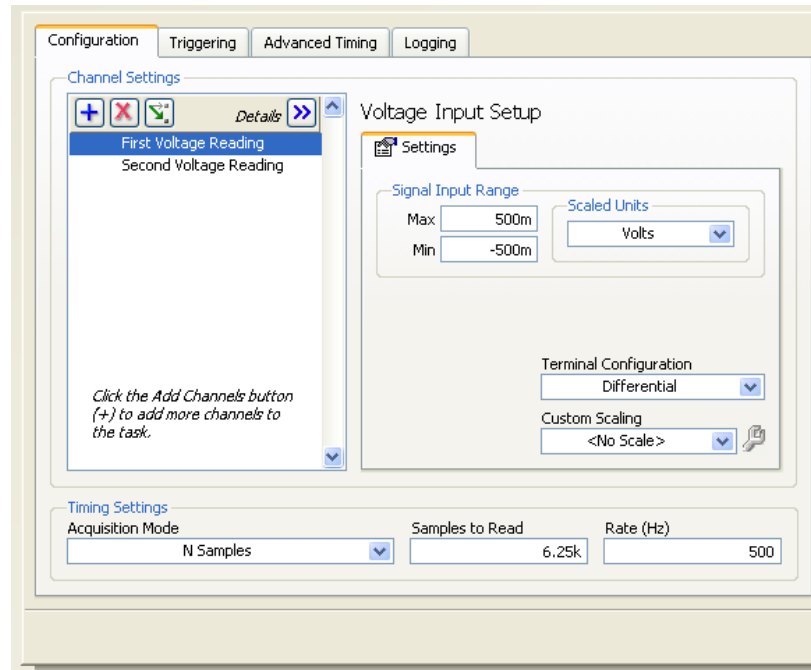


Figure 8 – LabVIEW's DAQ Assistant.

To collect a data sample, I set DAQ assistant to acquire to a selected number of points (i.e. 6250) with a selected acquisition rate (i.e. 500 Hertz). I set the rotation stage at about -20 degrees with 0 degrees being when the sample was about normal to the optical axis. The motion controller's rotation velocity was fixed at the selected speed (i.e. 2 degrees per second). The acceleration of the motion controller that brought the rotation to a constant velocity was set at 80.0 deg/s^2 . With these settings in place, I recorded the initial angle, and then ran the VI. I manually controlled the motion controller to rotate the sample from -20 degrees to 20 degrees. The DAQ collected the data for the intensity of the laser outputs, and I recorded the angle at which the rotation stopped. This is the procedure that I used to collect the data that is analyzed in the next section. The key equipment used in this experiment is listed in Table 1.

Description	Vendor	Model Number
External-cavity diode laser (780-nm)	New Focus	7013
External-cavity diode laser (1550-nm)	New Focus	7028
Tunable laser controller	New Focus	Vortex 6000
1310-nm diode laser	Thorlabs	ML725B8F
Laser diode controller	Thorlabs	LDC 210 C
700-1800-nm detector x2	Thorlabs	PDA10CS
Analog to digital converter	National Instruments	USB – 6009
Rotating step motor	Thorlabs	URS75PP
Motion controller	Newport	ESP 300

Table 1 – List of key pieces of equipment used.

Data and Results:

LabVIEW's raw data yields intensity per data point. I used Microsoft Excel to convert the data into intensity per angle, to find the point where the oscillations began, and to plot the intensity as a function of the angle. Figures 10 and 11 display the intensity versus angle graphs for the 780-nm laser and the 1310-nm diode laser, respectively.

The sample in this experiment has parallel sides and is surrounded by air, so it is modeled well by the thin film interference illustrated in Fig. 2. In accordance with the theory, the transmitted waves have an angle dependent phase difference which results in an interference pattern that alternates when the sample is rotated. This was observed in the oscillations of the intensity as a function of angle. These oscillations are shown in Fig. 10 and Fig. 11, where the incident angle of light on the sample is approximately zero when the light is at normal incidence to the sample.

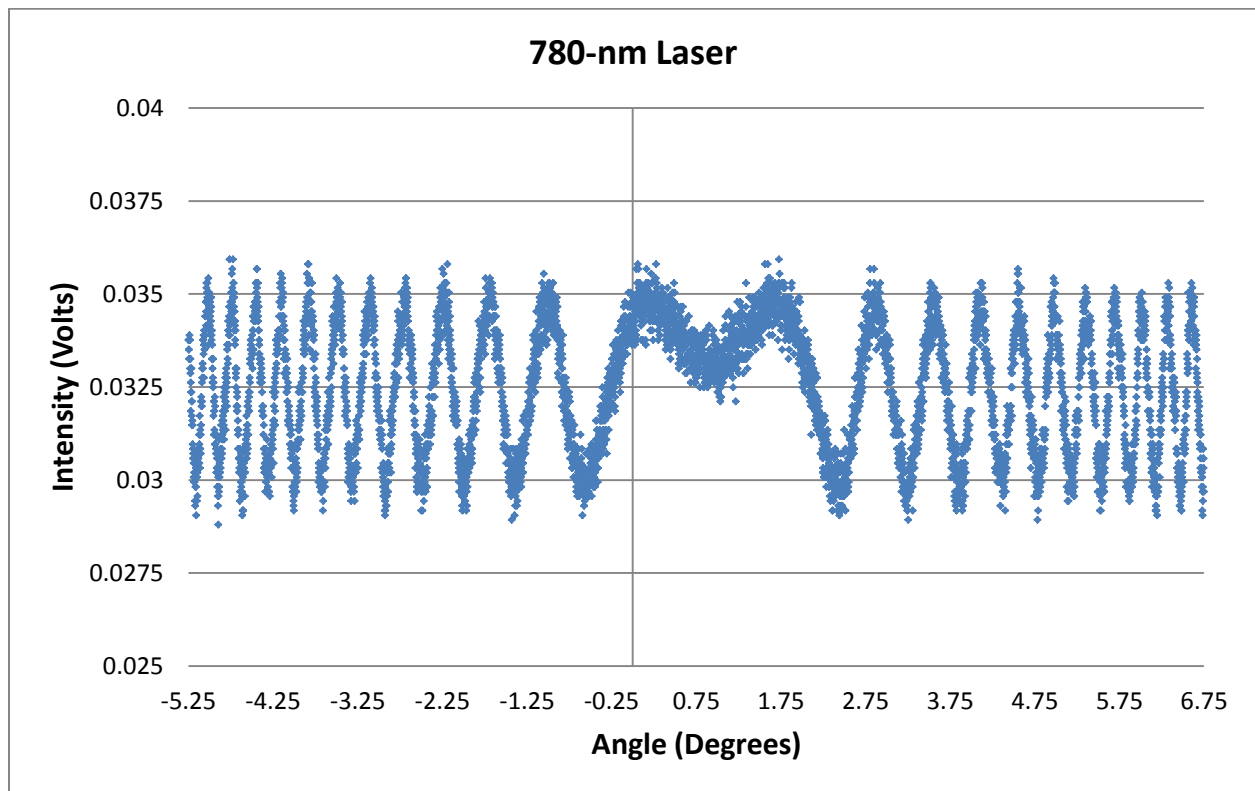


Figure 10 – The intensity versus angle for the 780-nm laser.

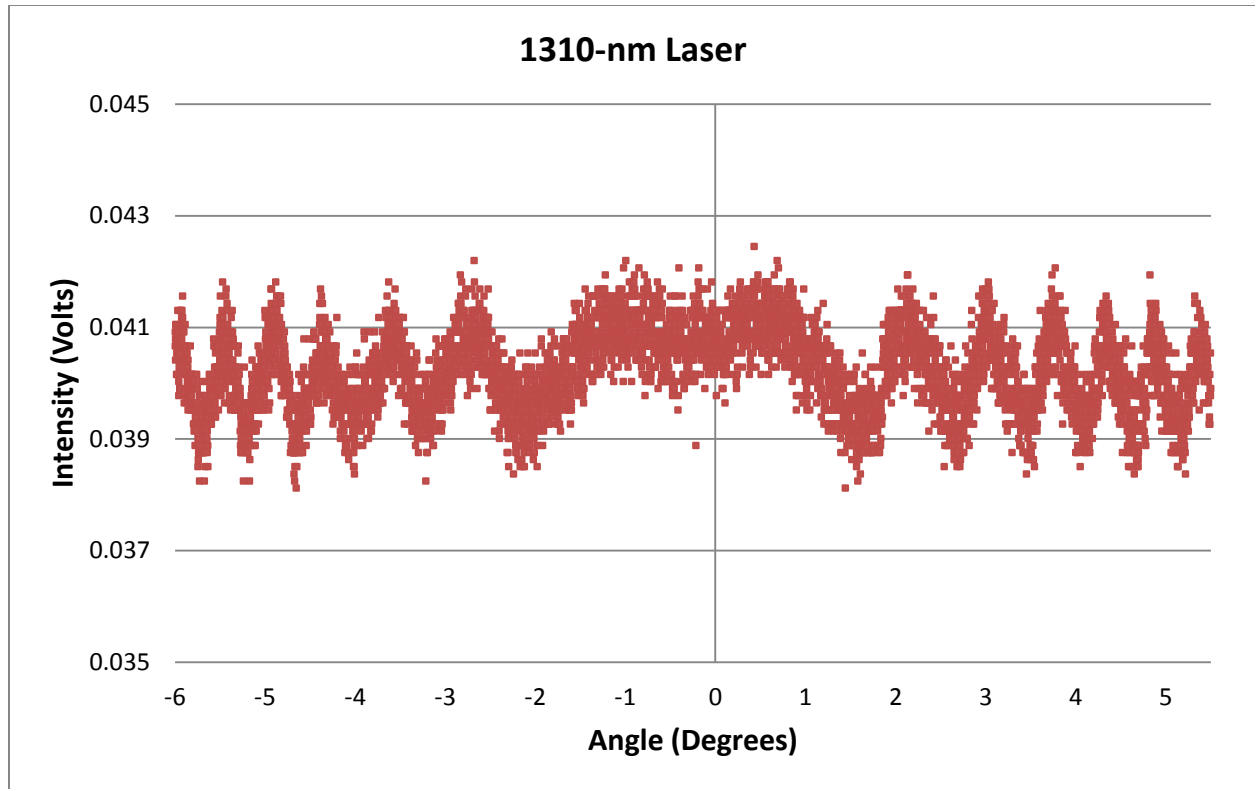


Figure 11 – The intensity versus angle for the 1310-nm diode laser.

For both lasers, the intensity was between the maximum and minimum when the incident angle of the light on the sample was zero. This is a consequence of the relationship between the optical distance of the light's path and its wavelength. From Eq. (4), the intensity is maximized when the cosine of the phase difference between transmitted waves is one. This occurs when the optical path difference of the transmitted waves is an integer multiple of the wavelength. Likewise, the intensity is minimized when the cosine of the phase difference is negative one. This occurs when the optical path difference is an integer multiple of the wavelength plus a half of a wavelength. When the optical path is at normal incidence to the sample, the optical distance of the transmitted light was neither a multiple of the wavelength nor a multiple of the wavelength

plus a half wavelength, so the graph showed the intensity to be in between the maximum and minimum.

Another feature of the intensities that Fig. 10 and Fig. 11 show is that the frequency of the oscillations increases as the angle from the normal increases in magnitude. This is because the rate of change of the phase difference increases as the sample angle increases. These results are expected due to the Fabry-Perot interference.

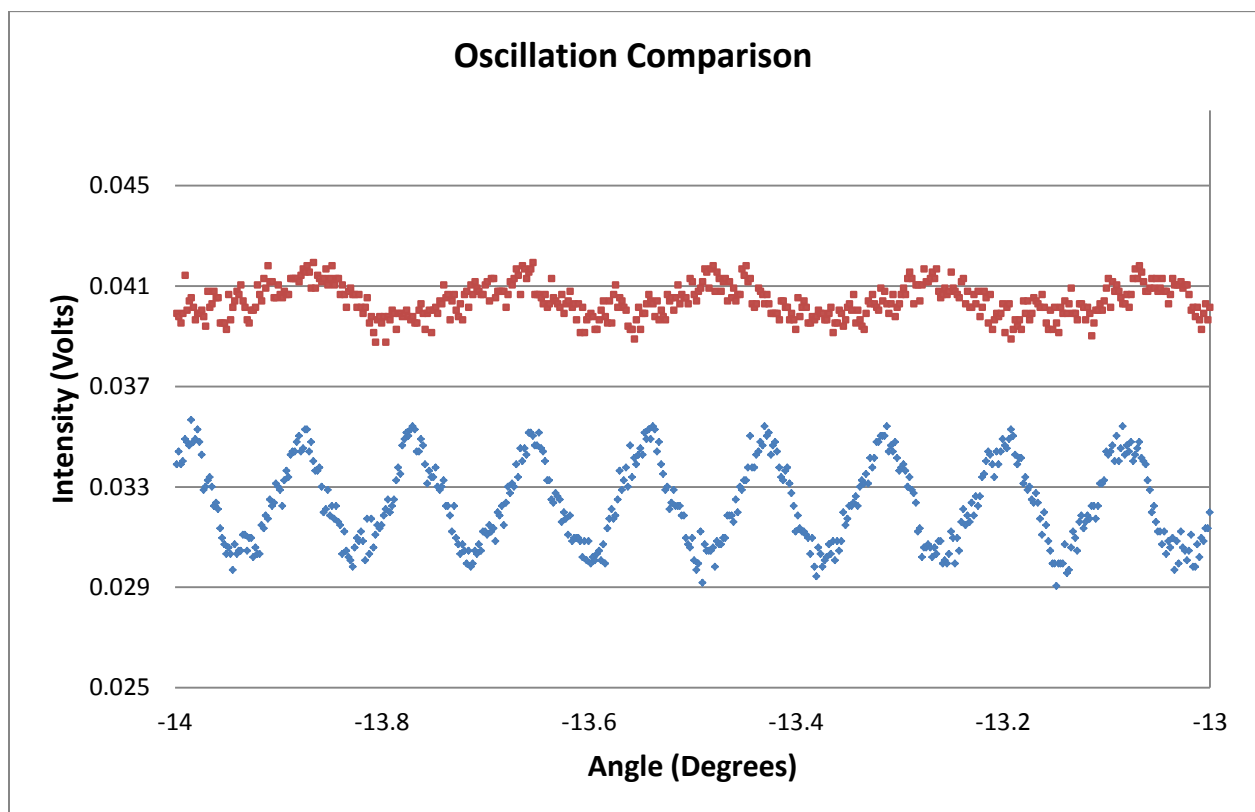


Figure 12 – The oscillations of the intensity for the 1310-nm laser (red) and the 780-nm laser (blue).

Furthermore, as seen in Fig. 12, we observed that the intensities oscillate at different frequencies. The 1310-nm light oscillates at a lower frequency than the 780-nm light. This is due to the wavelength dependence of the phase difference where the longer wavelength results in a lower frequency of oscillation. Figures 10, 11, and 12 are all from data that was taken with a rotation speed of two degrees per second. A faster rotation speed works just as well, and it allows for quicker scans.

Because the index of refraction depends on the wavelength, there is a slightly different measurement of the index of refraction for the two lasers. However, the thickness of the material is the same for both lasers. It is through the peak locations of the intensity that the refractive index and thickness are related and measured.

Conclusion:

This paper is a proof of theory for the dual-wavelength Fabry-Perot interferometric method. The oscillations of the intensity of the light as the sample was rotated are consistent with the results expected from Fabry-Perot interference.

Measuring the refractive index of thin infrared semiconductor materials proves to be a challenge. The physicists and engineers that have developed these experiments and the ones leading up to them demonstrate the ingenuity and creativity that practicing physics calls for. They model how the discipline of physics draws from both experiment and theory to build on what has come before it, and how technology is a both a useful tool and wonderful medium that allows physics to propagate.

Future Work:

The next step in this project would be to program LabVIEW to automate much of the data acquisition. A VI that reads, writes, and graphs the data for the intensity, controls the rotation stage, and converts the data to intensity versus angle would be a powerful improvement to this experiment. It would allow for samples to be analyzed rather quickly. Another improvement would be to design a method that efficiently changes the laser diodes out and aligns the new system. This would allow for more wavelengths to be tested on a sample to help construct a dispersion curve.

References

- [1] H. J. Choi, H. H. Lim, H. S. Moon, T. B. Eom, J. J. Ju, and M. Cha, "Measurement of refractive index and thickness of transparent plate by dual-wavelength interference," *Optical Express* **18** (9), 9429-9434 (2010).

- [2] Frank L. Pedrotti, Leno S. Pedrotti, and Leno M. Pedrotti, *Introduction to Optics*, Third Edition, (Pearson Prentice Hall, Upper Sadler River, NJ, 2007).

- [3] G.D. Gillen, and S. Guha, "Refractive-index measurements of zinc geranium diphosphate at 300 and 77 K by use of a modified Michelson interferometer," *Applied Optics* **43** (10), 2054-2058 (2004).

- [4] G.D. Gillen, and S. Guha, "Use of Michelson and Fabry-Perot interferometry for independent determination of the refractive index and physical thickness of wafers," *Applied Optics* **44** (3), 344-347 (2005).

- [5] Nicholas Czapla, "Building and Characterization of Laser Diodes as Well as System Design of a Dual-Wavelength Fabry-Perot Interferometer," Senior Project, Cal Poly, 1-34 (2012). <http://digitalcommons.calpoly.edu/physsp/55>

- [6] David J. Griffiths, *Introduction to Electrodynamics*, Third Edition, (Prentice-Hall, Inc., Upper Sadler River, NJ 1999).